Optical Sciences Center
University of Arizona
Tucson, Arizona 85721

DOUBLE ARCH MIRROR STUDY

PRELIMINARY ENGINEERING REPORT

Prepared for
NASA Ames Research Center
Space Technology Branch 244-7
Moffett Field, California 94035
January - March 1983

NASA Grant No. 2-220

by Daniel Vukobratovich

Principal Investigator
Don Hillman

CONTENTS

ILLUSTRATIONS

Figure

ILLUSTRATIONS--Continued

TABLES

Table

I. INTRODUCTION

An optical mirror mount must provide support without changing the optical figure of the mirror and must maintain the optical alignment of the mirror simultaneously. For the NASA Ames 20-in. double arch mirror, several environmental conditions affect the mount:

(a) Temperature: The mirror will be used at room temperature (75°F) and at cryogenic temperatures (-423°F).

(b) Pressure: Pressure will vary from sea level (14 psi) to vacuum.

(c) Gravity: The mirror will be tested in a 1-g gravity field and will be used in a weightless state. Steady-state launch loads of 3.2 g followed by gravity release must not alter alignment or mirror figure. An emergency landing load of 4.5 g must not damage the mirror and mount; realignment after such an incident is acceptable.

(d) Material: The mirror mount must provide a transition between the fused silica mirror and the aluminum telescope structure.

The NASA Ames 20-in. double arch mirror is shown in Fig. 1. (See Ref. 1 for a description of this mirror design.)

Several assumptions will be made in this report concerning this mirror:

(a) The mirror is assumed to be very stiff in its deformation behavior.

(b) The mirror is assumed to have a zero thermal coefficient of expansion.

(c) The tensile yield strength will be assumed to be 7100 psi (see Refs. 2, 3, and 4).

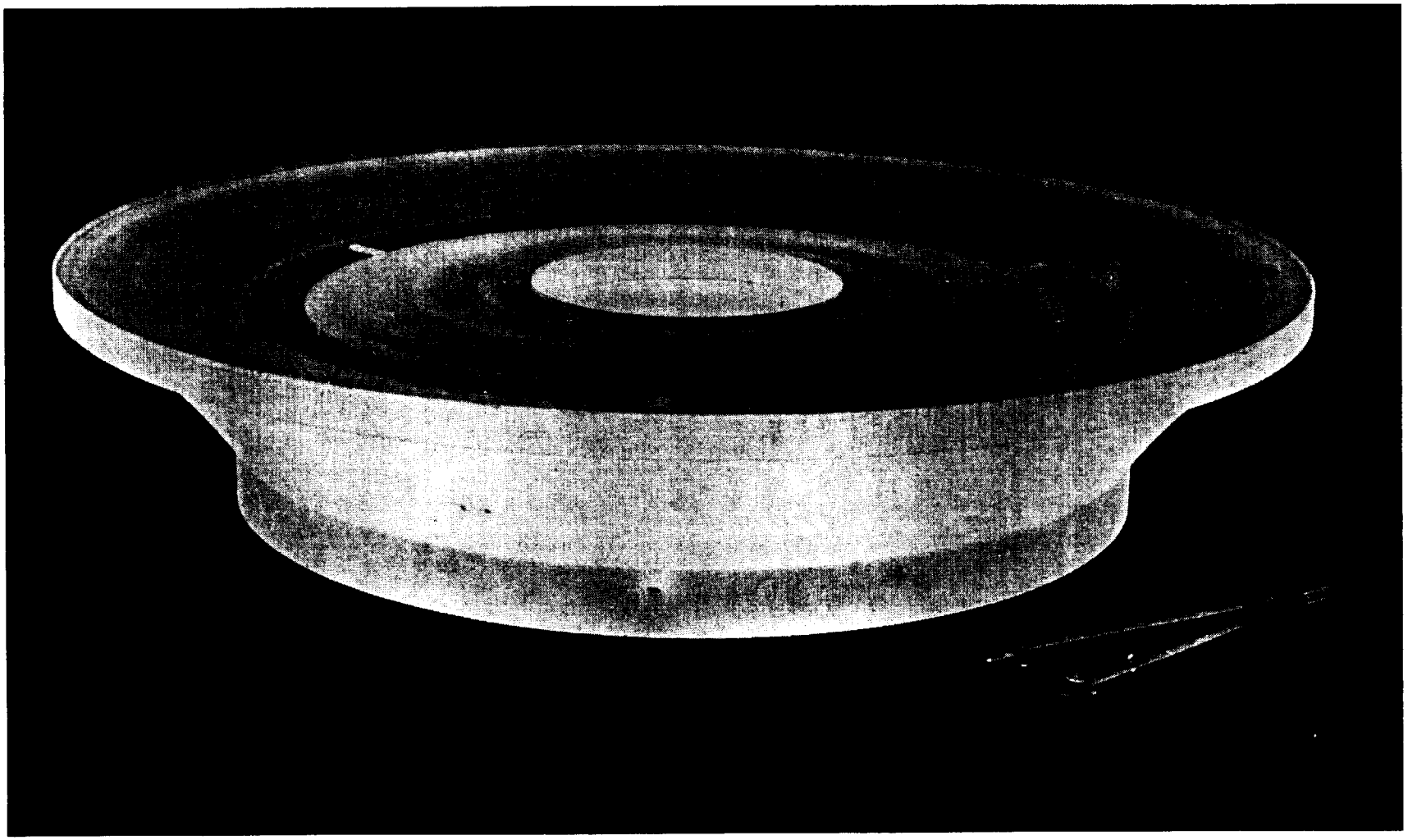

Fig. 1. NASA Ames 20-in. double arch mirror.

II. DESIGN CONCEPT

In the proposed design the mirror is supported by three clamp and flexure assemblies. The flexures are radially compliant but stiff in all other directions. These flexures allow the aluminum mirror cell to expand or contract relative to the mirror yet uniquely determine the position of the mirror. (See Figs. 2 and 3.)

The mirror clamp consists of a T-shaped Invar 36 member that goes into a similarly shaped socket in the back of the mirror (see Fig. 4). The mirror socket is made oversize and contacts the clamp only along the conical surface. The actual contact area is silver plated. The clamp is preloaded by a Belleville spring washer and pulls the mirror into contact with the flexure. The clamp is inserted into the mirror socket through a cutout, is rotated 90°, and then is pinned in place.

Because of the preload, the glass in the socket area is in compression. By adjusting the magnitude of this preload, the glass will remain in compression under all design loading conditions. This exploits the fact that glass is stronger in compression than tension. Since the socket is in the thickest part of the mirror, distortion of the optical figure due to clamping forces will be at a minimum.

Since Invar 36 has a greater thermal expansion than fused silica, the clamp will contract relative to the socket as the system is cooled. Since the clamp is under a preload and contacts only along the conical surface, a temperature change will maintain centration and simply change the actual contact area on the clamp.

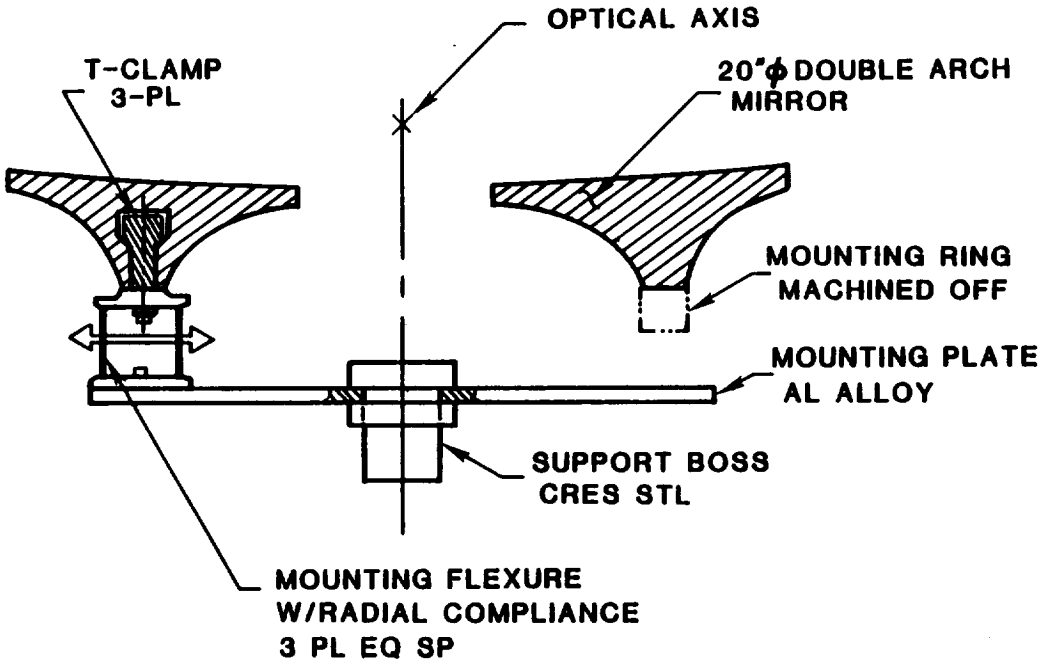

Fig. 2. Section through proposed mount.

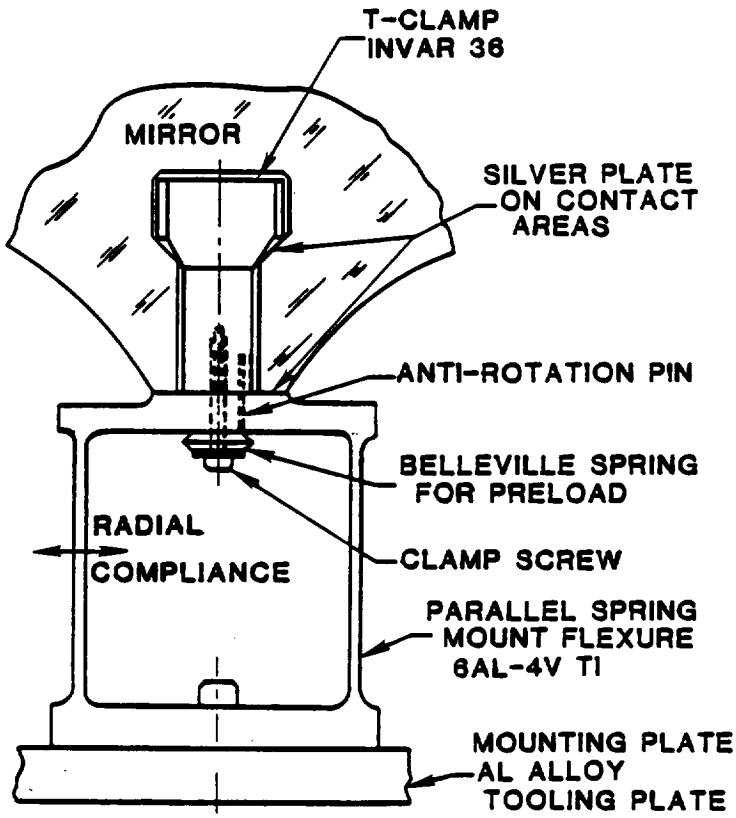

Fig. 3. Prime flexure mount assembly.

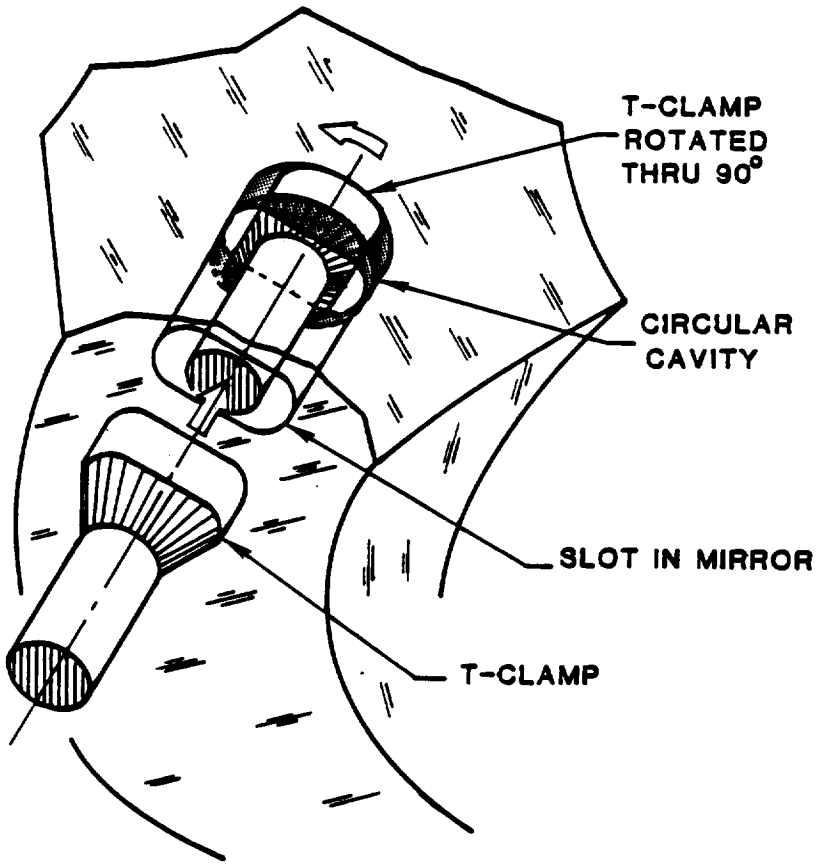

Fig. 4. Isometric view of T-clamp and slot.

The silver plate on the clamp acts to increase the contact area between clamp and socket. The silver plate also serves to reduce friction between clamp and socket. A Teflon washer is a possible alternative to the silver plate.

A similar clamp design was developed by the German Infrared Laboratory (GIRL). The GIRL mirror weighed 57 lb, which is 1-1/2 times the weight of the NASA Ames 20-in. double arch. During a shake table test of the GIRL system, the mirror supports failed before the clamps did (see Ref. 5).

The clamps are attached to flexures that are in turn attached to the mirror cell. These flexures are stiff in the axial and tangential directions but are compliant in the radial direction. By using three flexures, each with its radial compliance at 120° to the others, the mirror's position is uniquely determined without overconstraint. The radial compliance allows contraction of the mirror cell relative to the mirror without inducing a figure or alignment change.

The flexures take the form of parallel spring guides. In comparison with a single blade flexure, a parallel spring guide offers greater compliance (at equal length) and does not transmit a moment into the glass. The parallel spring guide also has greater stiffness and a higher fundamental frequency than a single blade flexure. The parallel spring guide is more sensitive to misalignment.

The chosen flexure material, a titanium alloy, allows the greatest compliance at cryogenic temperature without becoming excessively brittle. The titanium alloy has a relatively small change in size when cooled and is corrosion resistant.

The mirror mount plays no role in thermal control of the mirror. Since the mirror mount occupies a small fraction of the back of the mirror, access for thermal control is simplified.

III. SOCKET DESIGN

A. Loading Conditions

Figure 5 shows a section through the socket and clamp. The mirror weight is W and the shear force induced by the flexure is F. Note that the forces acting in the y axis do not affect the clamping surface.

Let F_N be the force normal to the clamping surface and let F_T be the force parallel to the clamping surface.

The greatest loads will be during an emergency landing with a cooled mirror. From NASA Ames information, the peak loads are

Direction	Load
z	$1/2\ \left(P + G\ \frac{W}{3}\right)$
x	$G\ \frac{\sqrt{2}}{2}\ W + F_F$

where G is the g-load.

Assume that the load is shared equally by both sides of the clamp. Then the maximum force normal to the clamping surface is

$$F_n = \frac{1}{2}\left(P + G\ \frac{W}{3}\right)\cos\theta + \left(G\ \frac{\sqrt{2}}{2}\ W + F_f\right)\sin\theta. \qquad (1)$$

The minimum force in the direction parallel to the clamping surface is

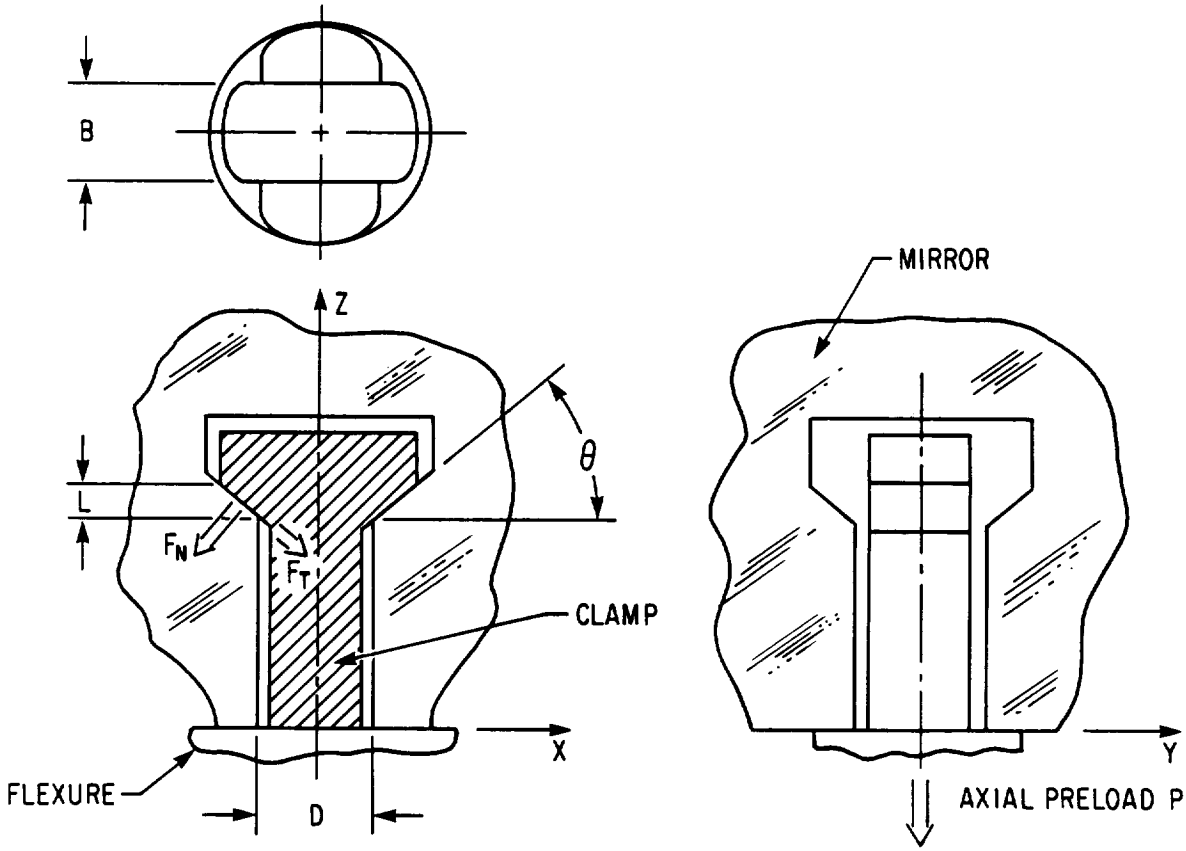

Fig. 5. Section through socket and clamp.

$$F_T = \frac{1}{2}\left(P + \frac{GW}{3}\right)\sin\theta - \left(G\,\frac{\sqrt{2}}{2} + F\right)\cos\theta\,. \qquad (2)$$

If the mirror is to remain aligned, the direction of the clamping force P must not change. Thus for the magnitude of P:

$$P \geq \frac{GW}{3}\,.$$

The flexure force F_F is to be determined using finite element methods. As an approximation, set F_F equal to the static load in a flexure when the mirror is on edge, or

$$F_F = \frac{\sqrt{2}}{2}\,W.$$

Then Eqs. (1) and (2) become

$$F_n = W\left[\frac{G}{3}\cos\theta + \frac{\sqrt{2}}{4}\,(G+1)\sin\theta\right] \qquad (3)$$

$$F_T = W\left[\frac{G}{3}\sin\theta - \frac{\sqrt{2}}{4}\,(G+1)\cos\theta\right]. \qquad (4)$$

B. Socket Stress in Emergency Landing

Assume that the socket and clamp are in perfect contact. Then the compressive stress σ_c is

$$\sigma_c = K\,\frac{F_n}{A}\,,$$

where K is a stress concentration factor and A is the contact area. The stress concentration factor may be determined by considering the socket geometry as the intersection of two cylindrical holes. (See Ref. 6). Peterson suggests a value for K of 4.7. The theoretical value of K for the intersection of a small hole into a large one would be 9. Since the socket is tapered, the angle of intersection is not as acute, and the lower value of K will be used.

The contact area A may be approximated by

$$A \cong \frac{BL}{\sin\theta} .$$

Then, using Eq. (3), the maximum compressive stress is

$$\sigma_c = \frac{KW \sin\theta}{BL} \left[\frac{G}{3} \cos\theta + \frac{\sqrt{2}}{4} (G+1) \sin\theta \right]. \qquad (5)$$

Let K = 4.7, W = 40 lb, G = 4.5. As an initial estimate, try B = 0.50 in., L = 0.25 in. Then Eq. (5) becomes

$$\sigma_{c_{G=4.5}} = 1504 \sin\theta(1.5 \cos\theta + 1.945 \sin\theta).$$

Now suppose that the value of G changes. Assume an equal change in both axes. For G = 2.0, Eq. (5) becomes

$$\sigma_{C_{G=2.0}} = 1504 \sin\theta(0.667 \cos\theta + 1.061 \sin\theta).$$

For G = 9.0, Eq. (5) becomes

$$\sigma_{C_{G=9.0}} = 1504 \sin\theta(3 \cos\theta + 3.536 \sin\theta) \cos\theta)].$$

The socket stress vs socket angle is calculated in Table 1.

Table 1. Socket Stress σ_c vs Socket Angle θ

θ (Degrees)	σ_c G=2.0 (psi)	σ_c G=4.5 (psi)	σ_c G=9.0 (psi)
5	99	218	432
10	220	474	932
15	358	760	1484
20	509	1067	2072
25	669	1386	2678
30	833	1708	3283
35	996	2022	3869
40	1153	2319	4419
45	1299	2590	4915
50	1430	2827	5342
55	1542	3072	5688
60	1631	3170	5942
65	1694	3266	6096
70	1731	3307	6146
75	1739	3293	6089
80	1719	3222	6089
85	1670	3098	5669
90	1595	2925	5317

It is seen that a change in the mirror weight W, contact area BL, or stress concentration factor K will simply multiply the values in the table. Thus for scaling these results to other mirror sizes while maintaining the same stress levels

$$\frac{W}{BL} = \text{constant} = 320.$$

C. Socket Stress in Cool-Down

Assume that cool-down is performed with the mirror in a face-down position on the ground. Then the peak loads are

Direction	Load
z	$1/2\ (P + \frac{W}{3})$
x	F_F

If the coefficient of friction between the socket and clamp is υ, then for the socket to be able to slip in order to reduce the shear stress:

$$\upsilon F_n < F_T . \tag{6}$$

Now

$$F_n = \frac{1}{2}\left(P + \frac{W}{3}\right)\cos\theta + F_F \sin\theta$$

$$F_T = \frac{1}{2}\left(P + \frac{W}{3}\right)\sin\theta - F_F \cos\theta.$$

Substituting into Eq. (6) and inserting the loads, for slipping to occur

$$\upsilon\left[\left(P + \frac{W}{3}\right) \cos\theta + F \sin\theta\right] - \left(P + \frac{W}{3}\right) \sin\theta - F_F \cos\theta = 0$$

or

$$\tan\theta = - \frac{\upsilon\left(\frac{G+1}{3}\right) + \sqrt{2}}{\upsilon \sqrt{2} - \frac{G+1}{3}} . \tag{7}$$

Table 2 shows the calculations for G = 4.5. The friction coefficients are from Ref. 7.

D. Stress due to Socket and Clamp Mismatch

If the angles of the socket and clamp differ, then true area contact will not occur. Instead, line contact will take place. This will raise the compressive stress.

Let $\Delta\theta$ be the difference in angle between the socket and clamp. The average radius R_s of the socket is

$$R_s = \frac{1}{2}\left[D + \frac{L}{\tan\theta}\right]. \tag{8}$$

The average radius R_c of the mismatched clamp is

$$R_c = \frac{1}{2}\left[D + \frac{L}{\tan\theta}\,(1-\Delta\theta)\right]. \tag{9}$$

The length C of the contact area will be

$$C = 2R_s \sin^{-1}\left(\frac{B}{2R_s}\right). \tag{10}$$

Table 2. Friction Coefficient ξ vs Minimum Socket Angle θ Required for Slip

υ (Friction coefficient)	θ (Degrees)
0.400	59.5
0.500	64.2
0.600	68.6
0.605 (hard steel on glass	68.8
0.675 (copper on glass)	71.7
0.700	72.6
0.721 (mild steel on glass)	73.4
0.775 (nickel on glass)	75.4
0.800	76.3
0.845 (aluminum on glass)	77.8
0.900	79.6
1.00	82.7

The normal force F_n is found using Eq. (3) (same assumptions as in section III-A). Using Hertz contact stress theory for the case of a cylinder in a cylindrical socket, the maximum compressive stress σ_c is

$$\sigma_c = 0.798K \left[\frac{R_s - R_c}{2R_s R_c} \frac{F_n/C}{\frac{1-\nu_s^2}{E_s} + \frac{1-\nu_c^2}{E_c}} \right]^{1/2}, \qquad (11)$$

where

K is the stress concencentration factor (assume 4.7 as in section III-B).

υ_s is the Poisson ratio for the socket material (0.17 for fused silica).

υ_c is the Poisson ratio for the clamp material (0.33 for Invar).

E_s is the elastic modulus for the socket material (10.6×10^6 psi for fused silica).

E_c is the elastic modulus for the clamp material (21.4×10^6 psi for Invar).

Let $\theta = 65°$, $G = 4.5$, and $W = 40$ lb. Then using Eq. (3), $F_n = 32.8$ lb. Now D must be greater than B if the clamp is to be inserted into the socket. Then try D = 0.56 in., B = 0.50 in., and L = 0.25 in. Then using Eqs. (8) and (11), $R_s = 0.338$ in. and S = 0.563 in. Table 3 shows σ_c calculated as a function of $\Delta\theta$ using Eq. (11).

Table 3. Socket Stress σ_c as a Function of Socket Angle Error $\Delta\theta$

$\Delta\theta$ (Degrees)	σ_c (psi)
0.001	165
0.01	523
0.1	1654
0.2	2339
0.3	2865
0.4	3309
0.5	3670
0.6	4054
0.7	4379
0.8	4682
0.9	4967
1.0	5236

Thus for a realistic assembly tolerance of 0.4° the stress is about the same as that calculated using the assumption of full area contact. Hertz contact theory becomes increasingly inaccurate as R_c approaches R_s,

so the very low values of σ_c for small $\Delta\theta$ should not be taken seriously. This suggests a "corrected" model that combines both theoretical approaches. See Fig. 6.

Introducing a soft material at the interface will have the effect of increasing the contact area and reducing the stress. Consider the use of a TFE plastic (Teflon) "washer" in the area of contact. From Refs. 8 and 9, for TFE, $\nu = 0.46$ and $E = 6.5 \times 10^5$ psi (at -423°F). Alternatively, the clamp could be silver plated. For silver, $\nu = 0.33$ and $E = 11 \times 10^6$ psi. As before, let $\theta = 65°$, G = 4.5, W = 40 lb, D = 0.56 in., B = 0.5 in., and L = 0.25 in. Then using Eq. (11) we can derive Table 4.

Table 4. Effect of Compliant Interface Material on Socket Stress σ_c

$\Delta\theta$ (Degrees)	σ_c (Teflon) (psi)	σ_c (silver) (psi)
0.001	14	39
0.01	45	123
0.1	141	387
0.2	199	548
0.3	244	671
0.4	282	775
0.5	313	860
0.6	345	950
0.7	373	1026
0.8	399	1097
0.9	423	1164
1.0	446	1227

These values for σ_c are below the 3300 psi stress arrived at using the assumption of full area contact. This means that the Hertz contact

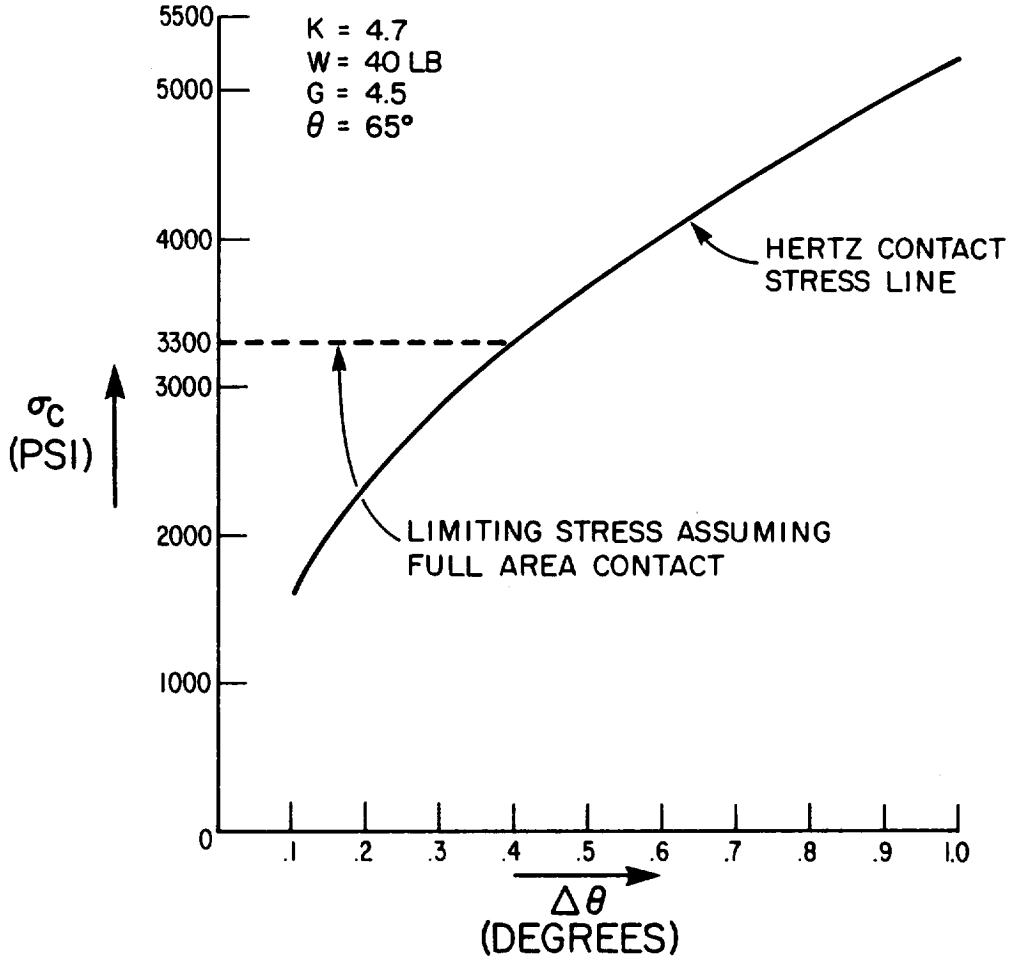

Fig. 6. Compressive stress vs socket angle error.

area would be larger than the assumed contact area. Since this cannot happen, if the clamp is Teflon coated or silver plated, it will be in full contact with the socket even for mismatched angles of 1°. Teflon cold flows at about 1000 psi at 76°F; this suggests that a Teflon-coated clamp would need to be periodically recoated.

E. Stress in Clamp

The T-shaped head of the Invar clamp may be modeled as a cantilever beam. The worst case would occur when the socket and clamp are angularly misaligned so that just the tip of the clamp contacts the socket. The bending geometry is shown in Fig. 7.

The bending stress σ_B in the cantilever is

$$\sigma_B = \frac{M}{S} .$$

The moment M is

$$M = \frac{1}{2} F_z x.$$

The section modulus S is

$$S = \frac{B}{6} (T + x \tan\theta)^2 .$$

Combining,

$$\sigma_B = \frac{3F_z x}{B(T + x \tan\theta)^2}. \qquad (12)$$

Suppose

$$F_z = P + G \frac{W}{3}$$

and

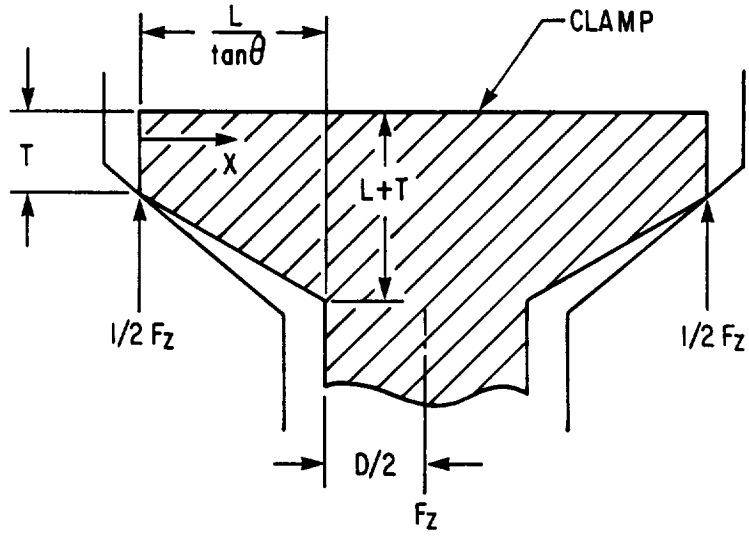

Fig. 7. Bending geometry of clamp.

$$P = \frac{GW}{3}.$$

Then Eq. (12) becomes

$$\sigma_B = \frac{2GWx}{B(T + x \tan\theta)^2}.$$

Differentiating and solving for x, the maximum stress will occur at

$$x = \frac{T}{\tan\theta}, \tag{13}$$

and Eq. (12) becomes

$$\sigma_{B_{max}} = \frac{GW}{2BT \tan\theta}.$$

Let B = 0.50 in., θ = 65°, G = 4.5, and W = 40 lb. Then using Eqs. (12) and (13), the maximum bending stress σ_{Bmax} is derived as shown in Table 5.

Table 5. Bending Stress as a Function of Clamp Edge Thickness

T (in.)	σ_{Bmax} (psi)
0.01	8394
0.02	4197
0.03	2798
0.06	1399
0.09	933
0.12	699
0.15	560
0.18	466
0.21	400
0.25	336

Since the microyield stress of Invar 36 is in the range of 10×10^3 to 25×10^3 psi (see Ref. 10), it is apparent that stress in the cantilever part of the clamp is not a problem.

Now consider the bending stress in the stem of the clamp. The geometry is shown in Fig. 8. The stem is kept in tension by the Belleville spring preload. The worst case bending moment is then

$$M = F_x(L + H).$$

This occurs when the socket angle is mismatched to the clamp such that contact occurs at the end of the clamp.

Assume that the stem has a circular cross section of diameter D. The section modulus S is then

$$S = \frac{\pi D^3}{32}.$$

Now using the same assumptions as in Sections III-A and III-B

$$F_x = G\frac{\sqrt{2}}{2}W + F_F = \frac{\sqrt{2}}{2}W(G+1).$$

Then maximum bending stress σ_s in the clamp stem is

$$\sigma_s = \frac{16\sqrt{2}\,W(G+1)(L+H)}{\pi D^3} + \frac{4GW}{3\pi D^2}. \qquad (14)$$

As before, let W = 40 lb, G = 4.5, L = 0.25 in.,and D = 0.56 in. Then using Eq. (14) we derive the results shown in Table 6.

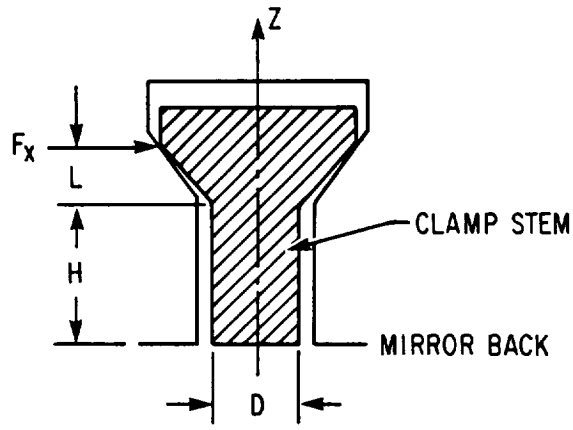

Fig. 8. Geometry of clamp stem.

The microyield stress of Invar 36 is in the range of 10×10^3 to 25×10^3 psi (see Ref. 10). To avoid microyield and the resulting need for realignment following an emergency landing, the stem length should be less than about 0.85 in. Invar has a yield point in the range of 40×10^3 to 60×10^3 psi, so a design based on a microyield stress of 10×10^3 psi will have a margin of safety of 4 to 6 in an emergency landing.

Table 6. Stem Bending Stress σ_s as a Function of Stem Length

H (in.)	σ_s (psi)
0.0	2500
0.2	4304
0.4	6109
0.6	7913
0.8	9718
1.0	11523
1.2	13372
1.4	15132
1.6	16936
1.8	18741
2.0	20545
2.2	22350
2.6	25959

F. Preload Spring

From sections III-A and III-B the preload force P is

$$P > \frac{GW}{3} .$$

For G = 4.5 and W = 40 lb,

$$P = 60 \text{ lb.}$$

For G = 1.0 and W = 40 lb,

$$P = 13.3 \text{ lb.}$$

From the Barnes spring catalog (Ref. 11) a type 302 stainless steel Belleville spring with this load capacity is available in part No. B0375-020-S. This spring will fit over a #10 screw. Due to hysteresis, a stacked Belleville spring configuration is not suggested.

G. Summary--Suggested Socket Design

Figure 9 is a schematic of the socket design. The maximum compressive stress in the glass for this design is found to occur during an emergency landing and is about 3300 psi. The preload is 60 lb. The maximum bending stress in the clamp is in the stem and again occurs during an emergency landing. This bending stress has a value of about 10×10^3 psi.

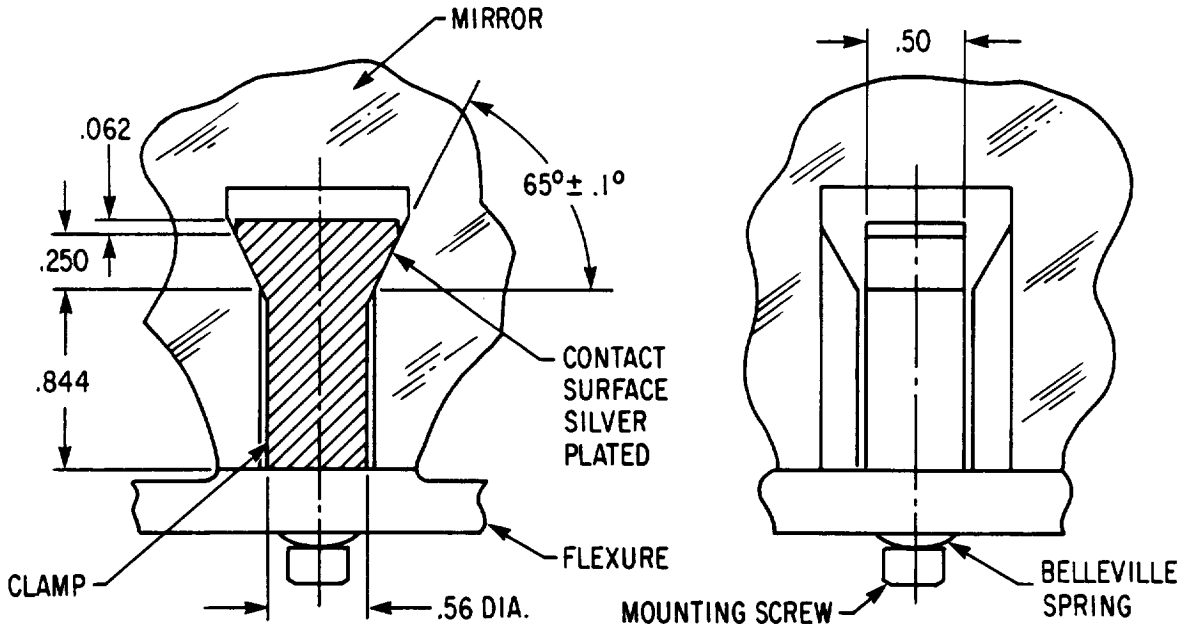

Fig. 9. Schematic of socket design.

IV. FLEXURE DESIGN

A. Flexure Geometry

Figure 10 is a schematic diagram of the flexure geometry.

B. Flexure Stress

The worst case loading for the flexure will be in the cooled condition during an emergency landing. From sections III-A and III-B:

$$F_z = P + G\frac{W}{3} = \frac{2GW}{3}$$

$$F_x = G\frac{\sqrt{2}}{2}W + F_F = \frac{\sqrt{2}}{2}W(G+1).$$

During a cool-down on the ground with the mirror in an inverted position, the flexures will be in tension. The loading then is

$$F_z = -\frac{W}{3}$$

$$F_y = F_F = \frac{\sqrt{2}}{2}W.$$

During launch the worst case loading would put the flexure into compression. Launch accelerations are lower than the emergency landing loads, but differ in magnitude depending on the axis.

Let G_{Lx} be the launch acceleration in the x direction and G_{Lz} be the launch acceleration in the z direction. Then the launch loads are

$$F_z = \frac{2G_{Lz}W}{3}$$

$$F_x = \frac{\sqrt{2}}{2}W(G_{Lx}+1).$$

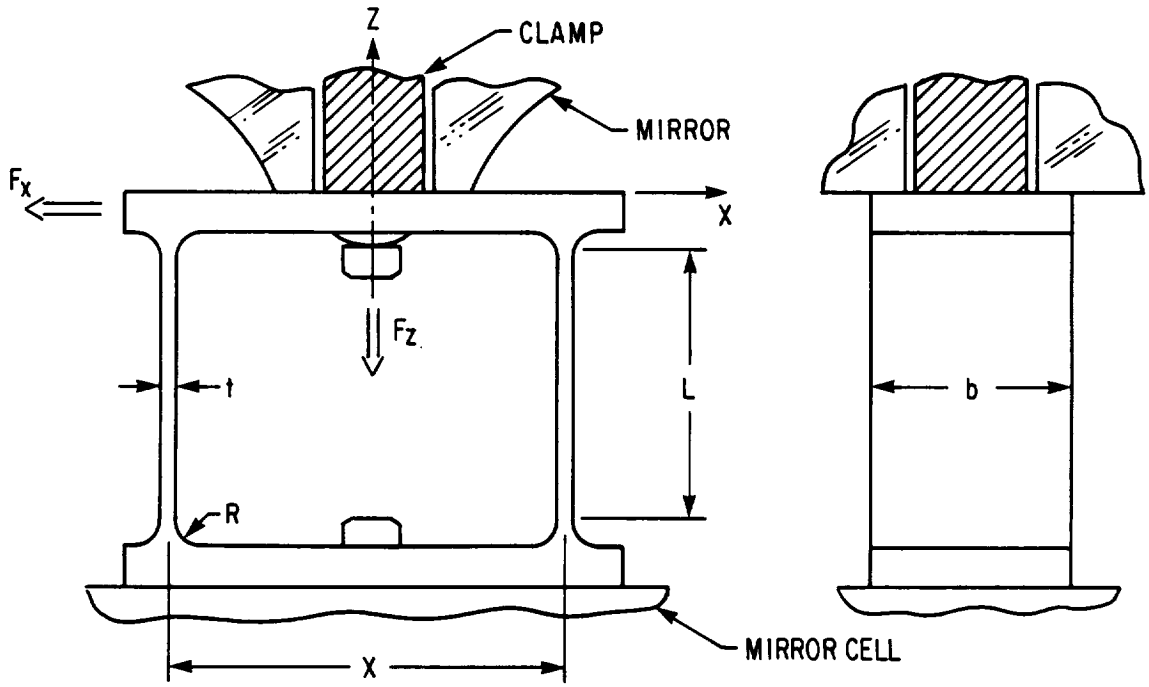

Fig. 10. Flexure geometry.

For alignment of the optical system to be maintained following launch, the maximum stress in the flexure must be less than the microyield stress of the flexure material. For the system to survive, maximum stress in flexure during an emergency landing should be less than the yield stress of the material.

The NASA Ames 20-in. double arch mirror has a mounting surface at a radius of 6.81 in. Assume that the mirror has a zero thermal coefficient of expansion. If the mirror cell is made of 6061 aluminum, the relative contraction of the cell to the mirror in cooling to -423°F is 0.0286 in. (see Ref. 9). The flexure must allow this much contraction while putting a minimum force into the mirror.

If the contraction is Δx, the flexural force F for a compressive loading is

$$F_F = \frac{F_z \Delta x}{L\left[\frac{\tan(nL/2)}{nL/2} - 1\right]} \tag{15}$$

where

$$n = \left(\frac{F_z}{2EI}\right)^{1/2}$$

E = flexure elastic modulus

I = moment of inertia of flexure section.

For a rectangular section

$$\frac{nL}{2} = \left(\frac{3F_z L^2}{2Ebt^3}\right)^{1/2}.$$

The maximum stress σ_F in the flexure for a compressive load is

$$\sigma_F = \frac{3F_f L}{2(nL/2)bt^2} \tan\left(\frac{nL}{2}\right) + \frac{F_z}{2bt} . \tag{16}$$

The choice of materials for the flexure is important. A good figure of merit for a flexural material is the reduced tensile modulus, which is defined as σ/E. To understand the importance of this ratio, consider a flexure where $F_z = 0$. Then Eqs. (15) and (16) become

$$F_F = \frac{24EI\Delta x}{L^3} \tag{17}$$

$$\sigma_F = \frac{F_F Lc}{4I} \tag{18}$$

where c is the distance to the neutral axis of the flexure.

From Eqs. (17) and (18)

$$\Delta x = \left(\frac{\sigma_F}{E}\right)\left(\frac{L^2}{6c}\right). \tag{19}$$

Thus for maximum flexural compliance, σ/E should be as large as possible. Secondary flexure material characteristics include a low thermal contraction in being cooled to -423°F and good impact strength at that temperature. See Table 7. Based on this table 6Al-4V ELI titanium will be the flexure material used.

The maximum allowable flexural stress σ_F will be the microyield stress of 6Al-4V ELI titanium. This was found to lie in the range of 48% to 53% of the 0.2% yield stress (see Refs. 10 and 12). Using the lower percentage, for 6Al-4V ELI titanium at -423°F (Ref. 9),

$$\sigma_F = (0.48)(240 \times 10^3 \text{ psi}) = 115 \times 10^3 \text{ psi}.$$

Equation (19) also shows that the optimum flexure has the greatest possible flexural length L and the smallest possible thickness. In this case, flexural length is constrained by buckling and by the height available in the NASA Ames cryostat. Assume that this height is 6.0 in.

Table 7. Metallic Flexure Materials for Cryogenic Applications

	$\frac{\sigma_{YS}}{E} \times 10^{-3}$		Thermal expansion (in./in.·F° x 10^{-6})	Thermal contraction $\frac{L_T - L_{68}}{L_{68}} \times 10^5$	Impact strength (ft-lb)
	At 68°F	At -425°F	at 68°F	at -423°F	at -423°F
Aluminum alloy 1100-H12	1.40	1.52	13.1	-390	40
Stainless steel 17-4 PH Cond. H1150-M	4.39	9.33	6.6	-190	5
Stainless steel type 304	1.25	2.07	9.6	-300	51
Titanium 6Al-4V ELI	7.27	15.0	5.3	-175	13
Titanium 5Al-2.5 Sn ELI	5.94	12.9	5.2	-175	8
Miraging steel 18 Ni (250)	9.25	12.9	5.0	-200	16
Invar 36 Ni	4.75	8.50	0.70	-60	20
Beryllium copper 1/2 hard	7.14	6.32	9.9	-320	30

The mirror is 3.0 in. thick with the mounting ring removed. Allow 1.0 in. for the mirror cell thickness and the flexure terminations. The remaining available flexural length is 2.0 in. This length is further reduced by the need to radius the transition at each end of the flexure to reduce stress concentration. Allowing for a 0.12 in. radius, the effective flexural length is 1.75 in.

The minimum thickness of the flexure is set by the difficulty of fabrication. From previous experience at the Optical Sciences Center, a reasonable minimum thickness t for the flexure is 0.050 in.

The above discussion leaves only the width b as a remaining degree of freedom in the design. The width chosen for b will depend on the loading condition.

The maximum flexural stress occurs at the ends of the flexure. There is a stress concentration at the transition which has the effect of lowering the allowable stress. From Ref. 6, this stress concentration factor K_F will be 1.5.

During launch $F_F = F_z$. There are two possible lift-off loadings:

	Case 1	Case 2
F_z	$G_{Lz}=3.2$	$G_{Lz}=0.8$
F_x	$G_{Lx}=0.8$	$G_{Lx}=3.2$

Then Eq. (16) becomes

$$\frac{\sigma_F}{K_F} = \frac{3F_xL}{2(\frac{nL}{2})bt^2}\tan(\frac{nL}{2}) + \frac{F_z}{2bt}$$

$$= \frac{3\sqrt{2}\ WL(G_{Lx}+1)}{2(nL/2)bt^2} \tan \frac{nL}{2} + \frac{G_{Lz}W}{3bt} . \qquad (17)$$

This equation can be solved for b. Let $E = 18 \times 10^6$ psi (at -423°F), L = 1.75 in., t = 0.050 in., W = 40 lb, $\sigma_F = 115 \times 10^3$ psi (at -423°F) and K_F = 1.5. Then for Case 1, b = 1.469 in. and for Case 2, b = 3.259 in.

In the case of zero gravity, Eqs. (17) and (18) apply. If b = 1.469 in., F_F = 35.3 lb. If b = 3.259, F_F = 78.3 lb. Although the finite element analysis has not yet been performed, these values for F_F are higher than the value suggested in Sections III-A and III-B. This suggests that a greater flexural length would be desirable. It is also seen that Case 2, where the greatest acceleration acts through the direction of flexural compliance, is the worst case.

Consider the use of a longer flexure. Let L = 2.50 in. All other parameters remain as before. Solving Eq. (17) for b: Case 1, b = 2.122 in.; Case 2, b = 4.678 in.

Then for zero gravity: Case 1, F_F = 17.5 lb; Case 2, F_F = 38.7 lb.

Lengthening the flexures reduces the load on the mirror due to cool-down. However, as the flexure lengthens, it also must become wider if alignment is to be maintained following launch. It is also apparent that the minimum flexure width is for Case 1, where the 3.2-g launch load is along the optical axis of the mirror. The effect of flexural length on the mirror load due to cool-down in a zero gravity environment is seen in Fig. 11.

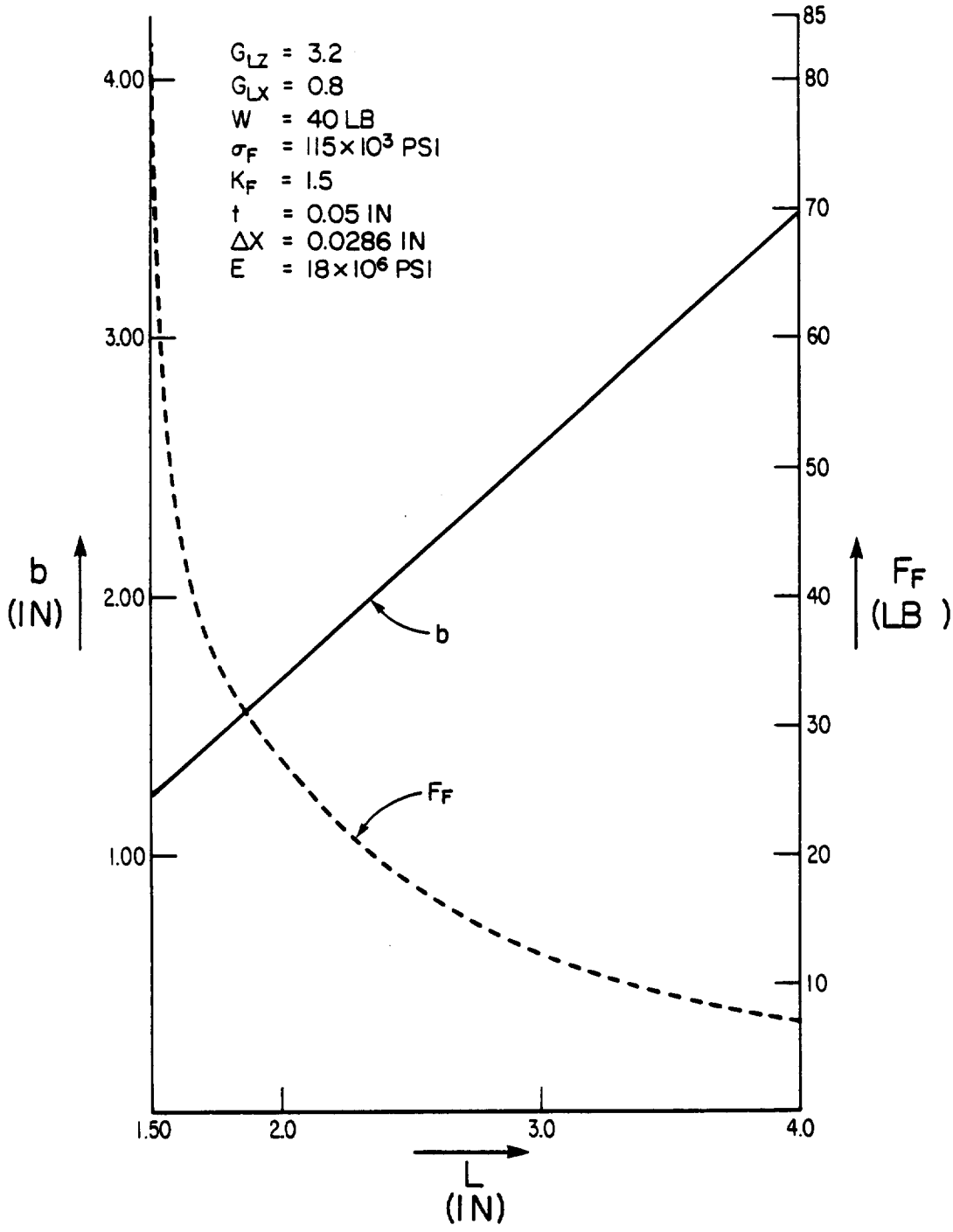

Fig. 11. Flexural force due to cool-down in zero gravity vs flexure length

Another way of increasing flexural compliance is to reduce the section thickness t. Let t = 0.040 in., L = 1.75 in., E = 18 × 10^6 psi (at -423°F), W = 40 lb, σ_F = 115 × 10^3 psi (at -423°F), and k_F = 1.5. Then for loading Case 1, b = 2.309 in., and F_F = 28.4 lb.

The flexure must also survive an emergency landing. Using the loads given in Sections III-A and III-B, Eq. (16) becomes

$$\sigma_F = K_F\left[\frac{3(G\,\frac{\sqrt{2}}{2}\,W + F_F)L\,\tan(\frac{nL}{2})}{2(\frac{nL}{2})bt^2} + \frac{GW}{3bt}\right].$$

Let G = 4.5, W = 40 lb, K_F = 1.5, and t = 0.05 in. Then for the previous flexure designs, Table 8 results.

Table 8. Flexure Stress σ_F for an Emergency Landing

L (in.)	b (in.)	F_F (lb)	σ_F (psi×10^3)
1.50	2.247	82.8	193
1.75	1.469	35.3	127
2.50	2.122	17.5	79.5
3.00	2.572	12.3	63.7
3.25	2.803	10.5	57.8
3.50	3.034	9.1	53.0
3.75	3.253	7.9	49.4
4.00	3.509	7.1	45.4

Since the 0.2% of yield stress for 6Al-4V titanium at -423°F is 240 × 10^3 psi, the flexures will survive an emergency landing. Note that the larger flexures offer an increased margin of safety.

C. Effect of Flexure Error

The most serious flexure error is nonparallelism of the flexures. If the flexures are not parallel, then when deflected Δx in the direction of compliance, a moment will be put into the mirror at the point of attachment. If ε is the parallel error and X is the flexure separation, the magnitude of this moment is

$$M = \frac{EbT\Delta x^2 \varepsilon X}{4L^3} . \tag{18}$$

Let $E = 18 \times 19^6$ psi (at -423°F), $t = 0.05$ in. $\Delta x = 0.0286$ in. (at -423°F) $X = 2.0$ in. and $\varepsilon = 0.001$ in. Then for the previous flexure designs, Table 9 results.

Table 9. Mirror Moment as a Function of Flexure Error

L (in.)	b (in.)	M (in.-lb)
1.50	1.247	0.136
1.75	1.469	0.101
2.50	2.122	0.050
3.00	2.572	0.035
3.25	2.803	0.030
3.50	3.034	0.026
3.75	3.253	0.023
4.00	3.509	0.020

The effect of these moments on the mirror's figure will not be known until the finite element analysis is performed.

D. Effect of Mirror Cell Error

The mirror cell may be tilted relative to the base of the mirror. Consider a tilt in the ZX plane, that is, in the radial direction. This will induce a moment M_R in the mirror. For a tilt of θ_R, this moment is

$$M_R = \frac{Ebtx^2\theta_R}{2L} \tag{18}$$

where θ_R is in radians.

Let $\theta_R = 0.001$ rad, $E = 18 \times 10^6$ psi (at -423°F), $t = 0.050$ in., $x = 2.0$ in. Then for the previous flexure designs, Table 10 results.

Table 10. Mirror Moment as a Function of Radial Cell Tilt

L (in.)	b (in.)	M_R (in.-lb$\times 10^3$)
1.50	1.247	1.496
1.75	1.469	1.511
2.50	2.122	1.528
3.00	2.572	1.543
3.25	2.803	1.552
3.50	3.034	1.560
3.75	3.253	1.561
4.00	3.509	1.579

This is a much larger moment than that due to a parallelism error in the flexure. The magnitude of this moment is relatively unaffected by the flexure dimensons. Again, the effect of this moment on the figure of the mirror must await finite element analysis.

Now consider a tilt in the YZ plane, or in the tangential direction. This will induce a moment M_T in the mirror and a shear F_s at the point of

flexure attachment. Now if the flexures have an F_z load in compression, for a tilt of θ_T, the moment M_T is

$$M_T = \frac{EI\lambda\theta_T}{2}\left[L\lambda/2/\left(2 - \frac{1\lambda}{\tan(1\lambda/2)}\right)\right], \tag{19}$$

where

$$I = \frac{tb^3}{6}$$

$$\lambda = \left[\frac{6F_x}{Etb^3}\right]1/2$$

θ_T is in radians.

Similarly, the shear force F_s is

$$F_s = \frac{F_z\theta_T}{2 - \frac{L\lambda}{\tan(L\lambda/2)}}. \tag{20}$$

Under conditions of zero gravity, these equations become

$$M_T = \frac{6EI\theta_T}{L} \tag{21}$$

$$F_s = \frac{12EI\theta_T}{L^2}. \tag{22}$$

Let θ_T = 0.001 rad, E = 18 × 10^6 psi (at -423°F), and t = 0.050 in. Then in a zero gravity condition, for the previous flexure designs, the results are obtained as shown in Table 11.

Table 11. Mirror Moment as a Function of Azimuthal Cell Tilt

L (in.)	b (in.)	M_T (in.-lb$\times 10^3$)	F_{s_3} (lb$\times 10^3$)
1.50	1.247	1.163	1.551
1.75	1.469	1.630	1.863
2.50	2.122	3.440	2.752
3.00	2.572	5.104	3.403
3.25	2.803	6.099	3.753
3.50	3.034	7.182	4.104
3.75	3.253	8.262	4.406
4.00	3.509	9.721	4.861

Again, these are relatively large moments. It may be necessary to remove these by use of additional flexures.

E. Summary--Flexure Design

No suggested flexure can be designed until the finite element analysis has determined the allowable forces and moments that the flexure may exert on the mirror.

It has been shown that the radial force exerted on the mirror by the flexure during cool-down can be reduced to about 7 lb per flexure. It has also been shown that a reasonable flexure can be designed that will endure launch loads without auxiliary caging and still maintain optical alignment following gravity release. The same flexure design is capable of surviving emergency landing loads, although the system would have to be realigned following such an event.

Errors in the parallelism of the flexures create a moment of less than 0.14 in.-lb per flexure in the back of the mirror. Tilt errors in the mirror cell relative to the back of the mirror put large moments into the mirror. A radial tilt error of 10^{-3} rad puts about a 1.5×10^{3} in.-lb moment into the back of the mirror. A tangential tilt of 10^{-3} rad puts moments of 2.3×10^{3} to 4×10^{3} in.-lb and shear forces of 1.50 to 4.0 lb into the mirror back depending on the flexure design. A more complex flexural configuration may be needed to reduce the magnitude of these moments.

REFERENCES

1. Vukobratovich, D., et al., "Optimum shapes for lightweighted mirrors," Proc. SPIE 332 (1982).

2. ESCO Products Inc., Optical Materials and Components Handbook.

3. Heraeus Amersil, Optical Fused Quartz and Fused Silica.

4. Dynasil Coporation of America, Fused Silica.

5. Schlegelmilch, R., et al., "GIRL-German Infrared Laboratory Final Report of the Telescope Study, Phase B," NASA TM-75911 (1981).

6. Peterson, R. E., Stress Concentration Factors (Wiley, New York, 1974).

7. Tomlinson, G. A., "A molecular theory of friction," Phil. Mag. 7, 905-939 (1929).

8. Dupont, Teflon-Mechanical Design Data.

9. Schwartzberg, F. R., et al., "Cryogenic Materials Data Handbook," AFML-TDR-280, National Technical Information Service (1970).

10. Marschall, C. W., and Maringer, R. E., Dimensional Instability (Pergamon Press, New York, 1977).

11. Barnes, Stock Springs Handbook.

12. Maringer, R. E., et al., "Stability of structural materials for spacecraft application," Bettelle-Columbus Laboratories, Final Report on NASA Contract NAS5-10267, 1968.